Vol. 6 No. 2, Dec. 2026

FUAM Journal of Pure and Applied Science

Available online at
www.fuamjpas.org.ng

An official Publication of
College of Science
Joseph Sarwuan Tarka University,
Makurdi.

FUAM Journal of Pure and Applied Science
© College of Science, Joseph Sarwuan Tarka University, Makurdi
https://fuamjpas.org.ng/
Vol.6 No. 2 Dec. 2026

Experimental design strategy to model the adsorption of toxic metals from industrial wastewater onto untreated Giri-clay-based adsorbent via response surface methodology

I[1*]. Asifau, I[2]. Omoniyi, I[1]. Kehinde, P.D[1]. Elaoyi, I.Z[2]. Yashim, A[3*]. Elebo

[1]Department of Chemistry, Faculty of Physical Sciences, Ahmadu Bello University, Zaria, Nigeria
[2]Federal Ministry of Innovation, Science and Technology, Abuja, Nigeria
[3]Department of Industrial Chemistry, Faculty of Sciences and Computing, Federal University of Applied Sciences Kachia, Nigeria
*Correspondence E-mail: abuchielebo@yahoo.com: asfauidrisnuhu@gmail.com

Received: 24/12/2025 **Accepted**: 16/02/2026 **Published online**: 17/02/2026

Abstract
This study aimed to gain a deeper understanding of the adsorptive properties of Giri natural clay, thereby expanding knowledge of novel adsorbents and facilitating the design of an optimal adsorption system. This study employed response surface methodology (RSM) to model and assess the adsorption of Cr^{6+} and Pb^{2+} from industrial wastewater using Giri-clay, a low-cost adsorbent. The Giri-clay-adsorbent was characterised comprehensively using Fourier transform infrared spectroscopy, Energy dispersive X-ray spectrometry, Scanning electron microscope and X-ray diffraction. The influence of four process variables: adsorbent dosage (A), initial metal concentration (B), solution pH (C), and contact time (D), was examined through a central composite design (CCD). Optimization of process variables identified that the highest Pb^{2+} removal of 83.76 % occurred at A = 32.50 mg, B = 62.50 mg L^{-1}, C = 8.00, and D = 45.00 min, while the maximum Cr^{6+} removal of 71.51 % was achieved at A = 77.50 mg, B = 87.50 mg L^{-1}, C = 8.00, and D = 45.00 min. A comparison between model predictions and experimental data yielded high correlation coefficients (R^2 = 0.9455 for Cr^{6+} and 0.7814 for Pb^{2+}), demonstrating that the developed models reliably predict toxic-metal removal by Giri-clay.
Keywords: Clay, Optimisation, DesignExpert, Adsorption, Wastewater

Introduction

In recent times, it has been established that effluents containing heavy metals require rigorous treatment before environmental discharge, since such contaminants and their chemical transformation products can exert pronounced toxic effects even at trace concentrations [1]. Adsorption is a widely recognised and effective strategy for remediating heavy metals from aqueous effluents. When the adsorption system is properly designed, considering factors such as adsorbent surface area, and pore size distribution, it can yield a high-quality treated effluent with significantly reduced contaminant concentrations [2].

However, compared to other treatment technologies such as chemical precipitation, ion exchange, membrane filtration, and oxidation processes, adsorption offers notable advantages in terms of efficiency, design flexibility and operational simplicity [3]. It can be implemented in batch or continuous flow configurations and easily scaled to accommodate varying treatment capacities. Moreover, adsorption processes can produce pollutant-free effluents suitable for reuse in industrial or municipal applications, contributing to water conservation and sustainability [2]. A key feature of adsorption is its reversibility, which allows for the regeneration of the sorbent material through desorption, which extends the lifespan of the adsorbent and may lead to significant reductions in operational costs over time [4].

Activated carbon is the most commonly employed adsorbent; however, its relatively high-cost limits broader application. Consequently, adsorbent selection must balance cost with adsorptive performance and availability, driving research toward materials that are both efficient and economical [5]. Numerous studies have reported the use of alternative adsorbents, including activated silica, wood waste, mud, and various clays. Clay minerals, in particular, are attractive because of their low cost, abundant natural occurrence, high surface reactivity, and inherent ion-exchange capacity. Recent investigations have highlighted their effectiveness for sequestering both inorganic and organic contaminants, with particular emphasis on heavy metals and clay interactions [6].

Giri-clay is a porous, high-surface-area material produced by intercalating soils into the interlamellar region of naturally occurring clay minerals. This intercalation expands the basal spacing, creating a stable, three-dimensional mesoporous network with tuneable pore dimensions, surface acidity, and redox functionality, thereby transforming abundant natural soils into high-value-added solids [7]. The adsorption performance

of a solid sorbent is governed primarily by its pore architecture and surface chemical nature. In particular, the pore-size distribution dictates both the efficiency and selectivity of adsorbate uptake, because it determines which molecular dimensions can access interior adsorption sites and how rapidly diffusion occurs within the porous network. Numerous clay-related adsorbents have been studied, such as light expanded clay aggregate [8], natural clay (sale-Morocco) [9], Algerian kaolinite clay [10], fuller's earth clay [11], chitosan-clay [12], and bentonite clay [13].

The objective of this work is to utilise untreated natural clay (Giri clay) directly as an adsorbent, thereby eliminating costly pre-treatment steps and reducing the overall expense of the lead and chromium removal from ternary wastewater by employing a response surface methodology strategy. In addition, the structural morphology of Giri clay was characterised by FTIR, SEM, and XRD.

Materials and methods

Adsorbent

The clay sample was obtained from a natural deposit located in Giri, along the Abuja-Lokoja, Nigeria. The clay was extracted with a shovel, placed in a sterile container, and transported to the laboratory. Upon arrival, the bulk clay was mechanically crushed and passed through a 60-mesh (250 µm) sieve. It was then subjected to four successive rinses with deionised water to remove dust and soluble impurities. Finally, the washed clay was dried in an oven at 120 °C for 48 h until a constant mass was achieved [8].

Adsorbate

A stock solution containing 1000 mg L^{-1} of Cr^{6+} and Pb^{2+} was prepared by dissolving 5.12 g of K_2CrO_4 (molar mass = 194.19 $gmol^{-1}$) and 1.60 g of $Pb(NO_3)_2$ (molar mass = 331.21 $gmol^{-1}$) in deionised water, and subsequently diluted to the required initial concentrations.

Experimental procedure

Batch adsorption experiments for the removal of Cr^{6+} and Pb^{2+} by Giri clay were conducted in 250 mL glass flasks as captured in the design template presented in Table 1. Aliquots of 10 - 100 mg of the clay were added to 50 mL of aqueous metal solution with an initial concentration (C_0) ranging from 50 to 100 mg L^{-1}. The solution pH was adjusted to the desired value using 1 M HNO_3 and NaOH. The flasks were then placed on a temperature-controlled shaker (25°C) and agitated at 100 rpm for 90 minutes to reach equilibrium. After filtration, the residual metal concentration in the solution was quantified by atomic absorption spectrophotometry (AAS) [13]. The amount of metal adsorbed per unit mass of clay at equilibrium, q_e (mg g^{-1}), was calculated as stated in Equation (1).

$$q_e = \frac{(C_1 - C_2)V}{M} \qquad (1)$$

Where q_e is the sorbed metal ions (mg/g), C_1 and C_2 are the first and final concentration of the metal ions (mg/L), V is the volume of the pollutant, and m is the quantity of sorbent (mg).

Table 1: Design template of factor-level range

Adsorption variables	Symbol	Unit	Factor level	
			-1	+1
Adsorbent dose	A	mg	10	100
Adsorbate concentration	B	mg/L	50	100
pH	C	-	2	10
Contact time	D	min	30	90

Response surface methodology

Response surface methodology (RSM) is a collection of mathematical and statistical techniques for assessing how multiple factors and their interactions influence a response variable [14]. It enables the development and optimisation of independent variables while minimising the number of experimental trials required. The approach involves three main steps: experimental design, response surface modelling, and optimisation. In this study, a Central Composite Design (CCD) was employed using Design-Expert software (version 2013, USA) [15]. The relationship between the response and the selected factors is represented by a quadratic polynomial equation captured in Equation (2).

$$y = b_o + \sum b_i X_i + \sum b_{ii} X_{ii} + \sum b_{ij} X_i X_j + \varepsilon \quad (2)$$

Where y defines the inhibition efficiency forecasted, b_o defines the constant term of the developed model, b_i, b_{ii}, b_{ij} are process variables, coefficients, and X_i, X_{ii}, X_{ij} denote the experimental data.

Characterisation of Giri-clay

The functional groups present in the clay were characterised using Fourier-transform infrared (FTIR) spectroscopy with a Model-FTIR8400S (Shimadzu Corp., Japan) over the 4000-500 cm^{-1} range. Crystallinity of the clay was evaluated by X-ray diffraction (XRD) on a Rigaku Ultima IV diffractometer operating at 40 kV and 30 mA, with the degree of crystallinity calculated as the ratio of crystalline reflection area to total area across the measured 2θ range. Surface morphology was examined by scanning electron microscopy (SEM) using a JSM-6490LA (Jeol, Japan).

Results and discussion

Adsorbent characterisation

FTIR

FTIR analysis of the clay was performed to identify the functional groups that can bind toxic metals, as depicted in Figure 1(a). The spectrum shows O-H stretching bands of adsorbed water at 3823 cm^{-1} and 3893.8 cm^{-1}, Si-O stretching peaks at 1975.5 cm^{-1} and 1638.3 cm^{-1}, an Al-O-H bending vibration at 998.9 cm^{-1}, and a water-bending mode at 1636.3 cm^{-1}. Strong peaks at 790.2 cm^{-1} and 745.5 cm^{-1} correspond to free silica or quartz. These

assignments indicate that hydroxyl, siloxane, and aluminol groups on the clay surface are the primary sites responsible for metal ion adsorption [11].

XRD

The XRD pattern of the clay, as captured in Figure 1(b), revealed a sharp and intense peak at specific 2θ values denoting some level of crystallinity. Kaolinite, as the major phase, showed reflections near 12.3° and 24.9° (2θ), while quartz impurities were observed near 20.8° and 26.6°, thereby confirming the clay's mineralogical composition and structural order [16]. The clay pattern constitutes a broad spacing connoting amorphous content. However, the sharpness and intensity of the peaks depict a high degree of crystallinity, which is linked to the adsorption propensity of the clay sample [17].

SEM

SEM analysis captured in Figure 1(c) revealed that the raw clay consists of porous, irregularly shaped particles with a mushroom-like morphology, indicating that the clay layers are not fully exfoliated but instead form aggregated structures [17]. These aggregates are composed of numerous flaky layers stacked tightly together, which improves the overall accessible surface area. Consequently, the stacked surface area and partially agglomerated nature of the raw clay result in significant physical adsorption capacity for heavy-metal ions, despite the presence of a porous network that can accommodate metal species [18].

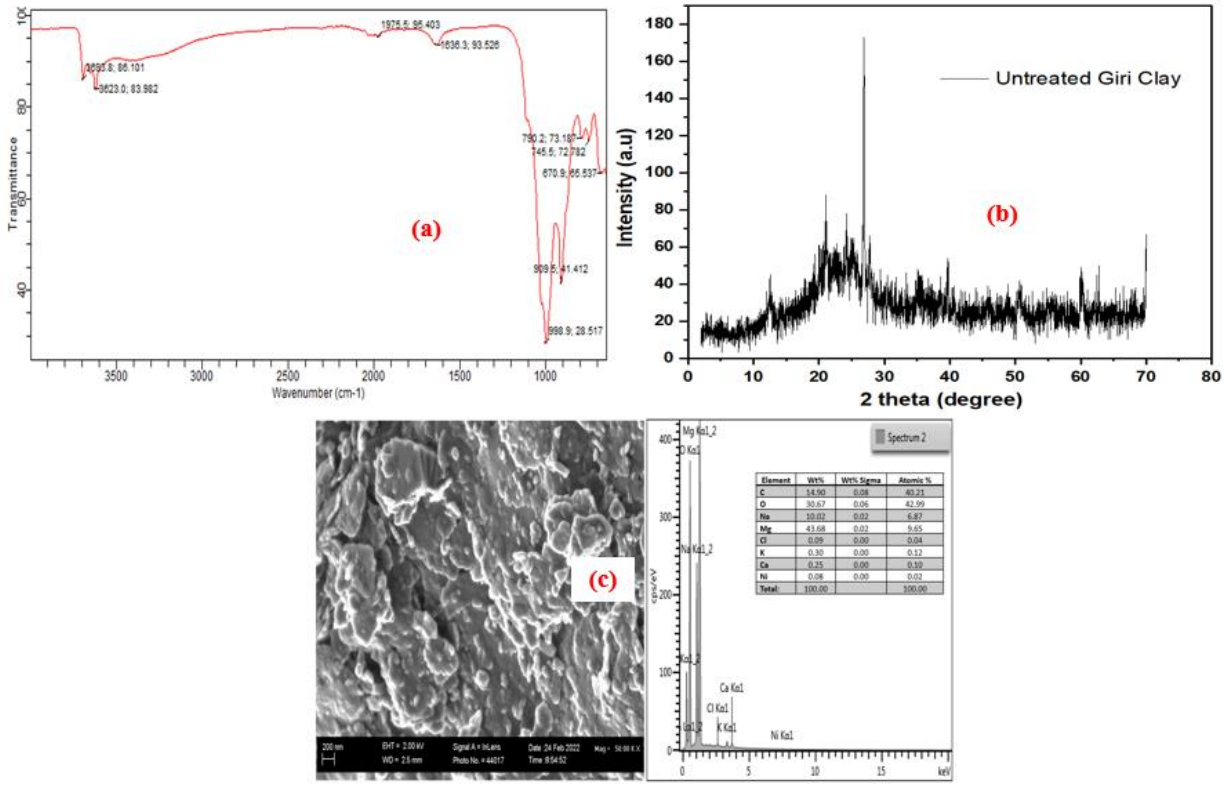

Figure 1: Characterisation of Giri-clay via (a) FTIR, (b) SEM, (c) XRD

Experimental design protocol

Sequel to the preliminary investigations, the independent variables selected for the adsorption study were initial metal ion concentration (Cr^{6+} and Pb^{2+}), solution pH, contact time, and adsorbent dosage. The response variable was the percentage removal of Cr^{6+} and Pb^{2+}. A five-level experimental design comprising 30 runs was employed, with the centre point replicated six times to estimate pure error. All trials were performed in duplicate, and the results are summarised in Table 2.

Optimisation revealed that the maximum Pb^{2+} removal of 83.76 % occurred at adsorbent dosage A = 32.50 mg, initial concentration B = 62.50 mg L^{-1}, pH C = 8.00, and contact time D = 45.00 min. For Cr^{6+}, the highest removal of 71.51 % was achieved at A = 77.50 mg, B = 87.50 mg L^{-1}, C = 8.00, and D = 45.00 min. However, similar maximum adsorption responses were reported by [1] and [14].

Table 2: CCD matrix of Cr^{6+} and Pb^{2+} adsorption onto Giri-clay

Run	A: Adsorbent (mg)	B: Adsorbate conc. (mg/L)	C: pH	D: Contact time	% Cr removal	% Pb removal
1.00	10.00	75.00	6.00	60.00	75.55	78.59
2.00	55.00	50.00	6.00	60.00	23.44	72.51
3.00	55.00	75.00	6.00	60.00	40.97	75.91
4.00	32.50	62.50	4.00	75.00	51.82	77.50
5.00	32.50	62.50	8.00	75.00	77.61	65.90
6.00	77.50	62.50	8.00	75.00	74.65	67.20
7.00	32.50	87.50	8.00	45.00	79.14	76.71
8.00	55.00	75.00	6.00	90.00	47.49	68.75
9.00	77.50	87.50	8.00	45.00	79.36	79.16
10.00	77.50	62.50	4.00	75.00	44.07	78.34
11.00	55.00	75.00	6.00	60.00	69.49	78.31
12.00	77.50	87.50	4.00	75.00	47.38	79.73
13.00	55.00	75.00	6.00	60.00	50.23	72.51
14.00	55.00	75.00	2.00	60.00	67.88	66.40
15.00	32.50	62.50	4.00	45.00	50.13	78.01
16.00	55.00	75.00	6.00	60.00	56.57	75.61
17.00	55.00	75.00	6.00	60.00	46.61	71.18
18.00	32.50	87.50	4.00	75.00	59.68	78.39
19.00	55.00	100.00	6.00	60.00	38.80	77.68
20.00	100.00	75.00	6.00	60.00	39.26	72.49
21.00	55.00	75.00	6.00	30.00	55.76	70.86
22.00	77.50	87.50	4.00	45.00	51.03	77.24
23.00	55.00	75.00	10.00	60.00	77.58	72.88
24.00	77.50	87.50	8.00	75.00	79.61	76.60
25.00	32.50	62.50	8.00	45.00	71.51	83.76
26.00	55.00	75.00	6.00	60.00	69.77	70.41
27.00	77.50	62.50	4.00	45.00	45.40	49.83
28.00	32.50	87.50	8.00	75.00	73.60	76.66
29.00	32.50	87.50	4.00	45.00	63.53	77.24
30.00	77.50	62.50	8.00	45.00	61.25	67.24

Statistical analysis

Since the full quadratic model is limited to meet adequacy criteria, it was refined by removing statistically insignificant terms, yielding reduced response-surface equations (Equations 3 and 4) that clearly illustrate the individual and interactive effects of the factors on Cr^{6+} and Pb^{2+} removal percentages. Analysis of variance (ANOVA) of these models (Tables 3 and 4) shows strong predictive capability, with adjusted R^2 values of 0.8420 for Cr^{6+} and 0.5774 for Pb^{2+}, and significant overall fit indicated by low p-values (<0.05) and F-values of 9.13 (Cr^{6+}) and 3.83 (Pb^{2+}). The lack-of-fit tests (Cr^{6+} $p = 0.3854$, Pb^{2+} $p = 0.0971$) confirm model validity. Coefficient estimates, standard errors, and term contributions reveal that all first-order main effects, especially adsorbent dosage (A), are highly significant, with initial metal concentration (B) exerting the greatest influence [19]. This finding is consistent with the report of [20] and [21], which employed biomass for the adsorption of toxic metal human blood plasma. Among second-order terms, pH (C) has the most pronounced effect on both responses, while the interaction between initial concentration and adsorbent dosage (D) is also highly significant [19].

Table 3: Analysis of variance (ANOVA) of Cr^{6+} adsorption

Source	Sum of Squares	df	Mean Square	F-value	p-value	Verdict
Model	5572.92	19	293.31	9.13	0.0005	Significant (**)
A-Adsorbent dose	36.39	1	36.39	1.13	0.3122	*
B-Adsorbate conc.	404.90	1	404.90	12.61	0.0053	**
C-pH	754.64	1	754.64	23.49	0.0007	**
D-Agitation time	44.59	1	44.59	1.39	0.2660	*
AB	33.15	1	33.15	1.03	0.3336	*
AC	123.48	1	123.48	3.84	0.0783	*
AD	285.81	1	285.81	8.90	0.0137	**
BC	476.11	1	476.11	14.82	0.0032	**
CD	316.67	1	316.67	9.86	0.0105	**
B^2	93.93	1	93.93	2.92	0.1180	*
C^2	210.39	1	210.39	6.55	0.0284	**
ABC	112.73	1	112.73	3.51	0.0905	*
ABD	310.45	1	310.45	9.67	0.0111	**
ACD	319.01	1	319.01	9.93	0.0103	**
BCD	1360.72	1	1360.72	42.36	< 0.0001	**
A^2B	70.18	1	70.18	2.18	0.1702	*
A^2C	185.49	1	185.49	5.77	0.0371	**
A^2D	64.56	1	64.56	2.01	0.1867	*
ABCD	270.38	1	270.38	8.42	0.0158	**
Residual	321.19	10	32.12			
Lack of Fit	89.36	5	17.87	0.3854	0.8406	not significant (*)
Pure Error	231.83	5	46.37			
Cor Total	5894.12	29				

R^2 = 0.9455, Adj. R^2 = 0.8420, Pred. R^2 = 0.5101, Adeq. precision = 10.1241

Table 4: Analysis of variance of Pb^{2+} adsorption

Source	Sum of Squares	df	Mean Square	F-value	p-value	Verdict
Model	2240.71	14	160.05	3.83	0.0071	Significant (**)
A-Adsorbent dose	83.16	1	83.16	1.99	0.1787	*
B-Adsorbate conc.	909.90	1	909.90	21.77	0.0003	**
C-pH	138.53	1	138.53	3.31	0.0887	*
D-Agitation time	11.22	1	11.22	0.2686	0.6119	*
AC	47.91	1	47.91	1.15	0.3012	*
BD	92.53	1	92.53	2.21	0.1575	*
CD	48.99	1	48.99	1.17	0.2960	*
B^2	166.91	1	166.91	3.99	0.0641	*
C^2	92.94	1	92.94	2.22	0.1566	*
D^2	201.35	1	201.35	4.82	0.0443	**
ACD	27.38	1	27.38	0.6553	0.4309	*
BCD	48.97	1	48.97	1.17	0.2961	*
A^2B	464.72	1	464.72	11.12	0.0045	**
ABCD	290.33	1	290.33	6.95	0.0187	**
Residual	626.82	15	41.79			
Lack of Fit	101.93	10	10.19	0.0971	0.9989	not significant (*)
Pure Error	524.90	5	104.98			
Cor Total	2867.53	29				

R^2 = 0.7814, Adj. R^2 = 0.5774, Pred. R^2 = 0.6018, Adeq. precision = 9.4486

$$\%\ \text{Cr removal/UTC} = +59.32 + 1.23A + 7.11B + 9.71C + 2.36D + 4.23AD + 5.45BC - 4.45CD - 2.72C^2 + 4.40ABD - 4.47ACD + 9.22BCD - 5.90A^2C - 4.11ABCD \quad (3)$$

$$\%\ \text{Pb removal/UTC} = +61.57 + 1.86A + 10.66B + 2.40C + 0.6838D - 2.75CD - 2.44B^2 + 1.82C^2 + 2.68D^2 - 9.33\ A^2B + 4.26ABCD \quad (4)$$

Optimisation of Cr^{6+} and Pb^{2+} adsorption studies

To elucidate the adsorption behaviour of Cr^{6+} and Pb^{2+}, three-dimensional response-surface plots were generated, each illustrating the influence of two variables on adsorption capacity while holding the remaining factors at their optimum levels (Figures 2 and 3). The dominant environmental parameters are adsorbate concentration and solution pH. Figures 2(a) and 2(b) depict the combined effects of Cr^{6+} concentration versus adsorbent dosage and agitation time versus pH on Cr^{6+} uptake, whereas Figures 3(a) and 3(b) show analogous interactions for Pb^{2+}. At a fixed pH, increasing the adsorbent dosage enhances metal-ion removal, which can be attributed to a greater number of accessible surface sites, increased metal-ion mobility, and pore-size modification of the sorbent [22]. Additionally, reduced fluid viscosity lowers resistance to intra-particle diffusion, further boosting capacity, a phenomenon reported for copper adsorption [10, 23, 24].

Conversely, at a given adsorbate concentration, raising the initial pH diminishes adsorption; at pH ≈ 4, competition between H^+ and metal ions (Cr^{6+}, Pb^{2+}) limits occupancy of active sites, thereby reducing uptake. The interaction between initial metal concentration and sorbent dosage (Figures 3(a) and 3(a)) shows that higher concentrations increase the concentration gradient, providing a stronger driving force that overcomes mass-transfer resistance and enhances adsorption [25]. However, increasing adsorbent dosage beyond a certain point lowers capacity, likely due to unsaturated surface sites and particle aggregation, which reduces available active area and lengthens diffusion pathways, a trend previously observed for hectorite clay-alginate composite beads for effective adsorption of methylene blue dye [26]. By applying response-surface methodology and optimisation, the maximum adsorption capacities achieved under varying parameters are summarised in Table 5.

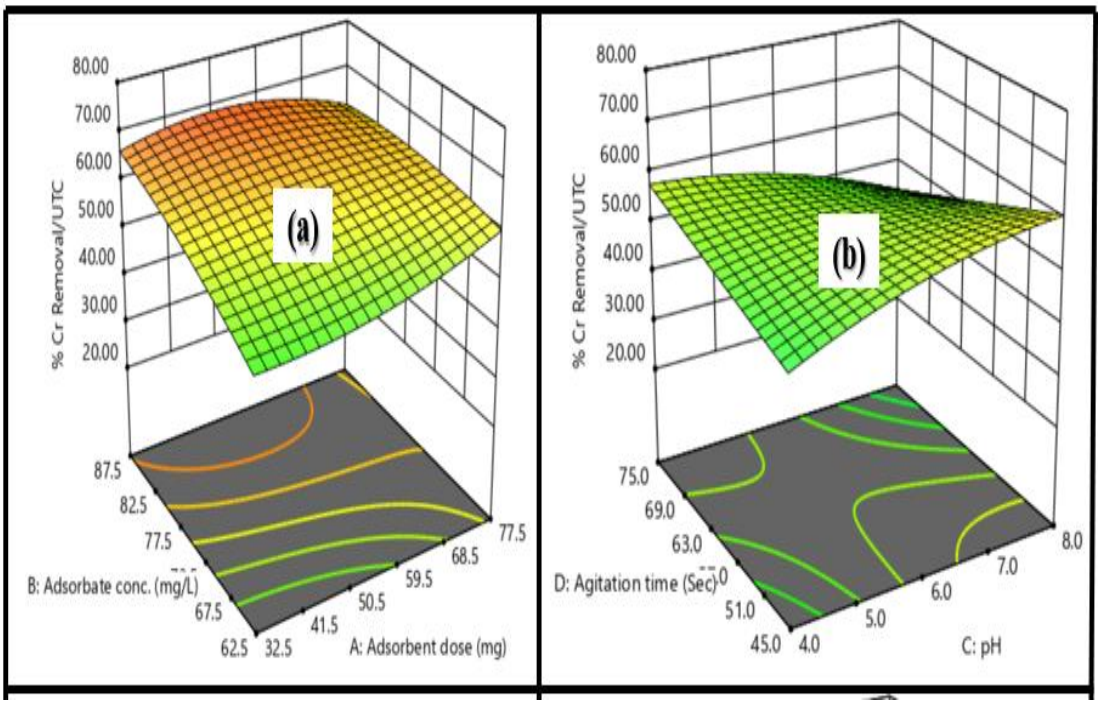

Figure 2: Three-dimensional plots of Cr^{6+} adsorption (a) adsorbate concentration versus adsorbent dose, (b) agitation time versus pH

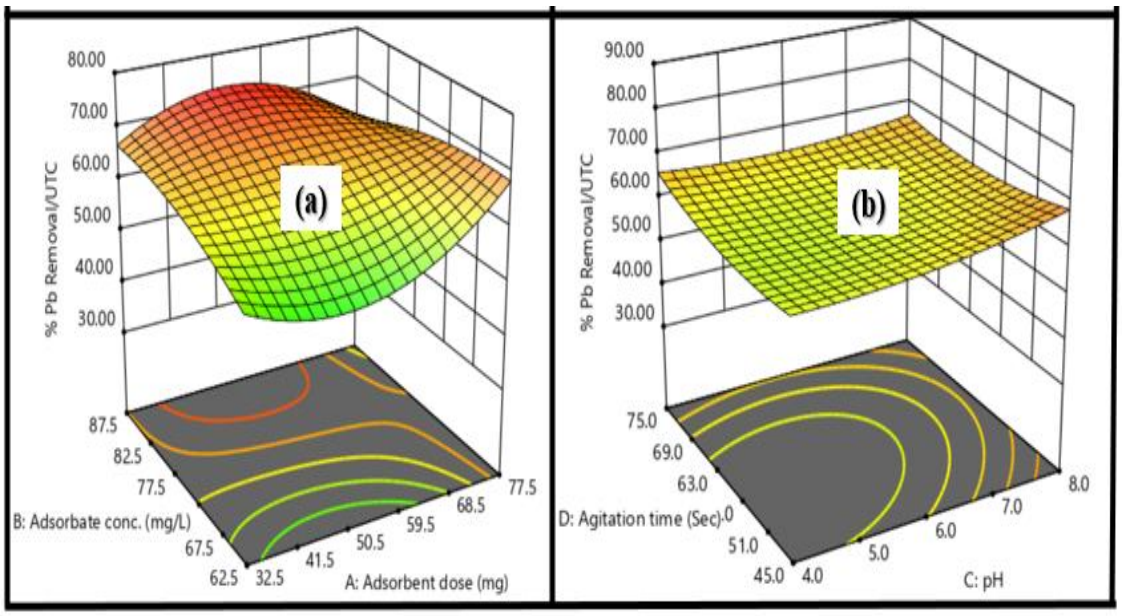

Figure 3: Three-dimensional plots of Pb^{2+} adsorption (a) adsorbate concentration versus adsorbent dose, (b) agitation time versus pH

Table 5: Suggested optimum adsorption conditions obtained via numerical optimisation

Toxic metal	A: Adsorbent (mg)	B: Adsorbate conc. (mg/L)	C: pH	D: Contact time (min)	% Removal
Cr (VI)	77.50	87.50	8.00	75.00	79.61
Pb (II)	32.50	62.50	8.00	45.00	71.51

Test and model validation

To validate the response-surface methodology (RSM) models, predicted (observed) values were compared with experimental measurements, yielding coefficients of determination (R^2) of 0.9455 for Cr^{6+} and 0.7814 for Pb^{2+}, as illustrated in Figure 5. The high R^2 values indicate that the models accurately capture the experimental trends, with data points closely aligned along the line of best fit [27, 28]. Additionally, analysis of externally studentized residuals plotted against experimental run order (Figure 5) shows no discernible outliers, confirming that the designated factor interactions reliably produce maximum adsorption of toxic metals from the ternary effluent [29].

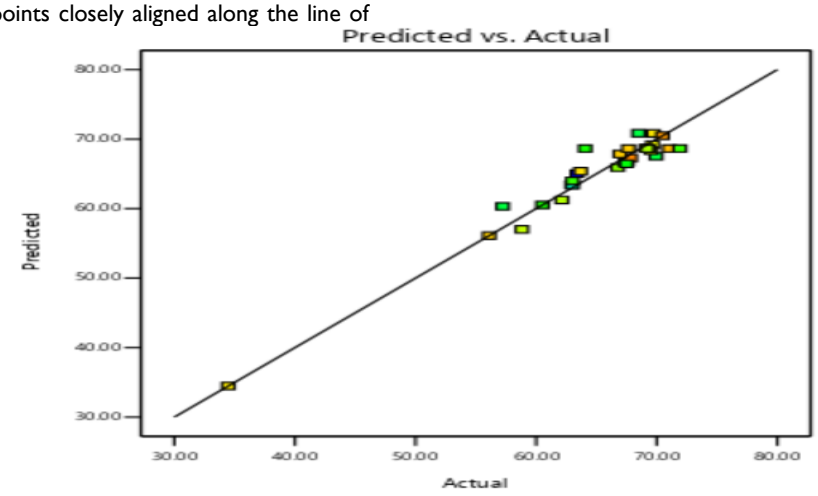

Figure 4: Diagnostic plot of predicted versus actual for Cr^{6+} and Pb^{2+} adsorption

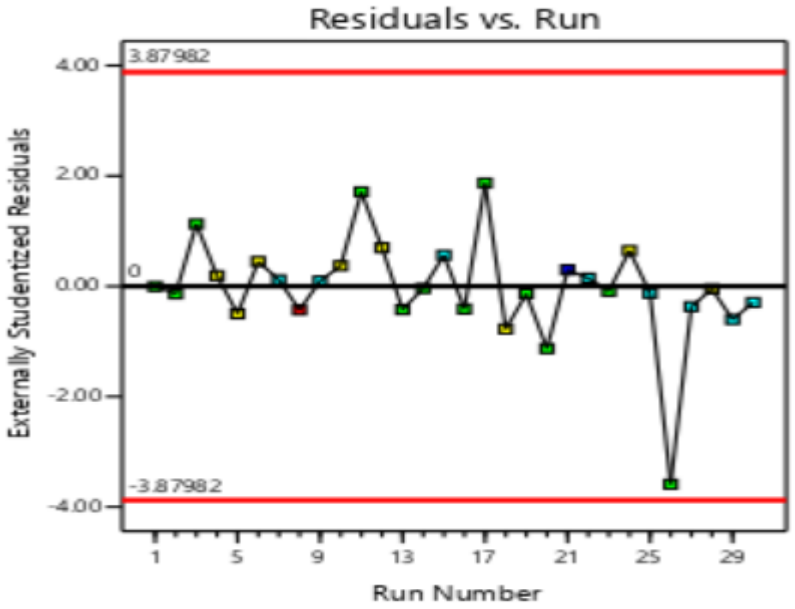

Figure 5: Diagnostic plot of residuals versus run for Cr^{6+} and Pb^{2+} adsorption

Conclusion

This research employed response surface methodology to examine the adsorption of Cr^{6+} and Pb^{2+} from aqueous solutions onto Giri-clay. The clay adsorbent was characterised by Fourier-transform infrared spectroscopy (FTIR), energy-dispersive X-ray spectrometry (EDX), scanning electron microscopy (SEM), and X-ray diffraction (XRD). SEM micrographs displayed a heterogeneous surface morphology with multiphase features, indicating a structure conducive to adsorption. The Cr^{6+} and Pb^{2+} were chosen to mimic textile-industry effluent containing toxic heavy metals. Characterisation of the adsorbent provided insight into the underlying adsorption mechanisms. Results showed that increasing both adsorbent dosage and initial metal-ion concentration enhanced Cr^{6+} and Pb^{2+} uptake. Consequently, Giri-clay demonstrates strong potential as an effective material for removing Cr^{6+} and Pb^{2+} from textile wastewater.

References

1. Elebo A, Ekwumemgbo PA, Elaoyi DP, Jibunor VU, Areguamen OI: **Isotherm and Kinetic investigations of toxic metal decontamination from biofluid by untreated biosorbent using a Batch design**. *Journal of Chemistry Letters* 2023, **4**(2):71-80.
2. Adeyemo AA, Adeoye IO, Bello OS: **Adsorption of dyes using different types of clay: a review**. *Applied Water Science* 2017, **7**(2):543-568.
3. Chai J-B, Au P-I, Mubarak NM, Khalid M, Ng WP-Q, Jagadish P, Walvekar R, Abdullah EC: **Adsorption of heavy metal from industrial wastewater onto low-cost Malaysian kaolin clay–based adsorbent**. *Environmental Science and Pollution Research* 2020, **27**(12):13949-13962.
4. Sellak S, Bensalah J, Ouaddari H, Safi Z, Berisha A, Draoui K, Barrak I, Guedira T, Bourhia M, Ibenmoussa S: **Adsorption of methylene blue dye and analysis of two clays: a study of kinetics, thermodynamics, and modeling with DFT, MD, and MC simulations**. *ACS omega* 2024, **9**(13):15175-15190.
5. Rao RAK, Kashifuddin M: **Adsorption studies of Cd (II) on Ball Clay: comparison with other natural clays**. *Arabian Journal of Chemistry* 2016, **9**:S1233-S1241.
6. Khenifi A, Bouberka Z, Sekrane F, Kameche M, Derriche Z: **Adsorption study of an industrial dye by an organic clay**. *Adsorption* 2007, **13**(2):149-158.
7. Elebo A, Sani U, Ekwumemgbo PA, Ajibola VO: **Green Synthesis and Zinc-Oxide Nanoparticles for Corrosion Inhibition and Modeling Corrosion Inhibition of Mild Steel in HCl Solutions**. *Biosensors and Nanotheranostics* 2024, **3**(1):1-17.
8. Shojaeimehr T, Rahimpour F, Khadivi MA, Sadeghi M: **A modeling study by response surface methodology (RSM) and artificial neural network (ANN) on Cu2+ adsorption optimization using light expended clay aggregate (LECA)**. *Journal of Industrial and Engineering Chemistry* 2014, **20**(3):870-880.
9. Es-Sahbany H, Hsissou R, El Hachimi M, Allaoui M, Nkhili S, Elyoubi M: **Investigation of the adsorption of heavy metals (Cu, Co, Ni and Pb) in treatment synthetic wastewater using natural clay as a potential adsorbent (Sale-Morocco)**. *Materials Today: Proceedings* 2021, **45**:7290-7298.
10. Rouibah K, Ferkous H, Abdessalam-Hassan M, Mossab BL, Boublia A, Pierlot C, Abdennouri A, Avramova I, Alam M, Benguerba Y: **Exploring the efficiency of Algerian kaolinite clay in the adsorption of Cr (III) from aqueous solutions: experimental and computational insights**. *Molecules* 2024, **29**(9):2135.
11. Kulkarni P, Watwe V, Chavan T, Kulkarni S: **Artificial Neural Networking for remediation of methylene blue dye using Fuller's earth clay**. *Current Research in Green and Sustainable Chemistry* 2021, **4**:100131.
12. Biswas S, Rashid TU, Debnath T, Haque P, Rahman MM: **Application of chitosan-clay biocomposite beads for removal of heavy metal and dye from**

industrial effluent. *Journal of Composites science* 2020, **4**(1):16.

13. Amin MT, Alazba AA, Shafiq M: **Adsorptive removal of reactive black 5 from wastewater using bentonite clay: isotherms, kinetics and thermodynamics**. *Sustainability* 2015, **7**(11):15302-15318.

14. Kumar ASK, Kalidhasan S, Rajesh V, Rajesh N: **Application of cellulose-clay composite biosorbent toward the effective adsorption and removal of chromium from industrial wastewater**. *Industrial & engineering chemistry research* 2012, **51**(1):58-69.

15. Dabagh A, Benhiti R, Mohamed E-H, Ait Ichou A, Abali Mh, Assouani A, Guellaa M, Berisha A, Hsissou R, Sinan F: **Application of Taguchi method, response surface methodology, DFT calculation and molecular dynamics simulation into the removal of orange G and crystal violet by treated biomass**. *Heliyon* 2023, **9**(11).

16. Islam MM, Islam MS, Maniruzzaman M, Haque MM-U, Mohana AA: **Banana rachis CNC/Clay composite filter for dye and heavy metals adsorption from industrial wastewater**. *Engineering Science & Technology* 2021:44-56.

17. Hernández-Montoya V, Pérez-Cruz MA, Mendoza-Castillo DI, Moreno-Virgen M, Bonilla-Petriciolet A: **Competitive adsorption of dyes and heavy metals on zeolitic structures**. *Journal of environmental management* 2013, **116**:213-221.

18. Dasgupta S, Das M, Klunk MA, Xavier SJS, Caetano NR, Wander PR: **Copper and chromium removal from synthetic textile wastewater using clay minerals and zeolite through the effect of pH**. *Journal of the Iranian Chemical Society* 2021, **18**(12):3377-3386.

19. Zhao H, Xie M, He S, Lin S, Wang S, Liu X: **Development of a novel nanoclay-doped hydrogel adsorbent for efficient removal of heavy metal ions and organic dyes from wastewater**. *Gels* 2025, **11**(4):287.

20. Uba S, Elebo A, Ekwumemgbo PA, Ajibola VO: **Application of CCD-RSM Strategy to Forecast Corrosion Inhibition of Expired Erythromycin on Mild Steel in Diverse Optimized HCl Concentration**. *Records of Chemical Sciences* 2024, **3**(1):16-22.

21. Olusegun SJ, de Sousa Lima LF, Mohallem NDS: **Enhancement of adsorption capacity of clay through spray drying and surface modification process for wastewater treatment**. *Chemical Engineering Journal* 2018, **334**:1719-1728.

22. Abu T, Adegoke H, Odebunmi E, Shehzad M: **Enhancing adsorption capacity of a kaolinite mineral through acid activation and manual blending with a 2: 1 clay**. *Nigerian Journal of Technological Development* 2024, **21**(1):131-151.

23. Sdiri A, Higashi T, Hatta T, Jamoussi F, Tase N: **Evaluating the adsorptive capacity of montmorillonitic and calcareous clays on the removal of several heavy metals in aqueous systems**. *Chemical Engineering Journal* 2011, **172**(1):37-46.

24. Prakash N, Latha S, Sudha PN, Renganathan NG: **Influence of clay on the adsorption of heavy metals like copper and cadmium on chitosan**. *Environmental Science and Pollution Research* 2013, **20**(2):925-938.

25. Oskui FN, Aghdasinia H, Sorkhabi MG: **Modeling and optimization of chromium adsorption onto clay using response surface methodology, artificial neural network, and equilibrium isotherm models**. *Environmental Progress & Sustainable Energy* 2019, **38**(6):e13260.

26. Pawar RR, Ingole PG, Lee S-M: **Use of activated bentonite-alginate composite beads for efficient removal of toxic Cu2+ and Pb2+ ions from aquatic environment**. *International Journal of Biological Macromolecules* 2020, **164**:3145-3154.

27. Badawi AK, Abd Elkodous M, Ali GA: **Recent advances in dye and metal ion removal using efficient adsorbents and novel nano-based materials: an overview**. *RSC advances* 2021, **11**(58):36528-36553.

28. İyim TB, Güçlü G: **Removal of basic dyes from aqueous solutions using natural clay**. *Desalination* 2009, **249**(3):1377-1379.

29. Rasilingwani T, Gumbo J, Masindi V, Foteinis S: **Removal of Congo red dye from industrial effluents using metal oxide-clay nanocomposites: Insight into adsorption and precipitation mechanisms**. *Water Resources and Industry* 2024, **31**:100253.

Cite this article

Asifau I., Omoniyi I., Kehinde I., Elaoyi P.D., Yashim I.Z., Elebo A. (2026). Experimental design strategy to model the adsorption of toxic metals from industrial wastewater onto untreated Giri-clay-based adsorbent via response surface methodology. FUAM Journal of Pure and Applied Science, **6**(**2**):41-49